THE JOURNAL OF PHYSICAL CHEMISTRY B

Article

pubs.acs.org/JPCB

Physicochemical Properties of Tri-*n*-butylalkylphosphonium Cation-Based Room-Temperature Ionic Liquids

Kazuki Yoshii,[†] Keisuke Yamaji,[†] Tetsuya Tsuda,*[,†] Katsuhiko Tsunashima,[‡] Hiroyuki Yoshida,[§] Masanori Ozaki,[§] and Susumu Kuwabata*[,†]

[†]Department of Applied Chemistry, Graduate School of Engineering, Osaka University, 2-1 Yamada-oka, Suita, Osaka 565-0871, Japan

[‡]Department of Material Science, Wakayama National College of Technology, 77 Noshima, Nada-cho, Gobo, Wakayama 644-0023, Japan

[§]Division of Electrical, Electronic and Information Engineering, Graduate School of Engineering, Osaka University, 2-1 Yamada-oka, Suita, Osaka 565-0871, Japan

ABSTRACT: The physicochemical properties of novel four tri-*n*-butylalkylphosphonium-based room-temperature ionic liquids (RTILs), tri-*n*-butylmethylphosphonium dimethylphosphate ($[P_{4,4,4,1}][DMP]$), tri-*n*-butyl(2-hydroxymethyl)phosphonium bis(trifluoromethylsulfonyl)amide ($[P_{4,4,4,2OH}][Tf_2N]$), tetra-*n*-butylphosphonium *O*,*O*′-diethylphosphorodithioate ($[P_{4,4,4,4}][DEPDT]$), and tri-*n*-butyldodecylphosphonium 3,5-bis(methoxycarbonyl)benzenesulfonate ($[P_{4,4,4,12}][MCBS]$), were examined in this study. All RTILs showed a favorable thermal decomposition temperature exceeding 560 K. Of these, $[P_{4,4,4,12}][MCBS]$ exhibited a fairly high thermal stability compared with common phosphonium cation-based RTILs reported to date. Interestingly $[P_{4,4,4,1}][DMP]$ formed an ionic plastic crystal phase within a range of 279−290 K, but that was not the case with $[P_{4,4,4,4}][DEPDT]$, which is similar in the cation and anion structures to the $[P_{4,4,4,1}]^+$ and $[DMP]^-$. $[P_{4,4,4,2OH}][Tf_2N]$ showed a relatively high conductivity of 0.48 mS cm^{-1} at 303 K among the RTILs consisting of tri-*n*-butylalkylphosphonium cation and usual fluoroanion.

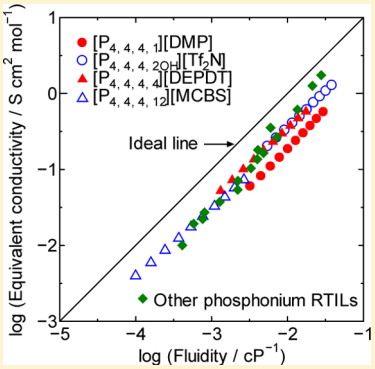

1. INTRODUCTION

Room-temperature ionic liquid (RTIL), which is a liquid salt at or below 293 K, has been investigated in the various scientific and industrial fields, such as energy technology, surface finishing, organic and inorganic synthesis, gas separation and vacuum technologies.[1−11] Multiplicity of the RTIL-related science and technology should be due to the RTIL's peculiar physicochemical properties including relatively high ionic conductivity, favorable thermal and chemical stability, wide electrochemical window, flame retardation, and negligible vapor pressure. Since the milestone papers on RTILs with fluoroanions were reported by Wilkes et al. and Cooper et al. in early 1990s,[12,13] numerous RTILs that can be handled easily under open-air condition have been reported.[14] In many cases, such RTILs consist of one onium cation species, such as imidazolium, pyridinium, ammonium, piperidinium, pyrrolidinium, phosphonium, and sulfonium, and one stable anion species in air. Another fascination of RTILs is that we can control their physicochemical properties by designing the ionic structure and changing the combination of cation and anion.[15−21]

Physicochemically stable quaternary phosphonium cation is recognized as one of the promising cation components in RTIL. The advantage is that various phosphorus salts with ordinary anions are commercially available and are produced in large quantity. Once phosphorus salts with halide anions such as Cl^- and Br^- showed a melting point above room temperature,[21] but now we can prepare many phosphonium cation-based RTILs by the combination with phosphonium cations and a wide variety of polyatomic anions, for example, bis(trifluoromethylsulfonyl)amide ($[Tf_2N]^-$), tetrafluoroborate ($[BF_4]^-$), dicyanamide ($[N(CN)_2]^-$), and fluorohydrogenate ($[(FH)_nF]^-$ ($1 \leq n \leq 3$)).[22−37] This RTIL system also has interesting features like other RTIL systems. For example, the combination of tetra-*n*-butylphosphonium ($[P_{4,4,4,4}]^+$) and amino-acid-based anion generates chirality-induced RTILs,[26] and the mixture of tetra-*n*-butylphosphonium hydroxide and benzimidazole can produce both hydroxide ion- and proton-conductive RTILs by controlling the mixing ratio.[27] Some phosphonium cation-based RTILs can form an ionic plastic crystal phase that is expected to be a next-generation electrolyte.[28,29] In this study, thermal stability and physicochemical properties of four types of the distinctive tri-*n*-butylalkylphosphonium-based RTILs depicted in Figure 1 were carefully investigated, and the thermodynamic data estimated from these data are discussed by comparison with those for other RTILs reported so far.

Received: July 9, 2013
Revised: October 6, 2013
Published: November 18, 2013

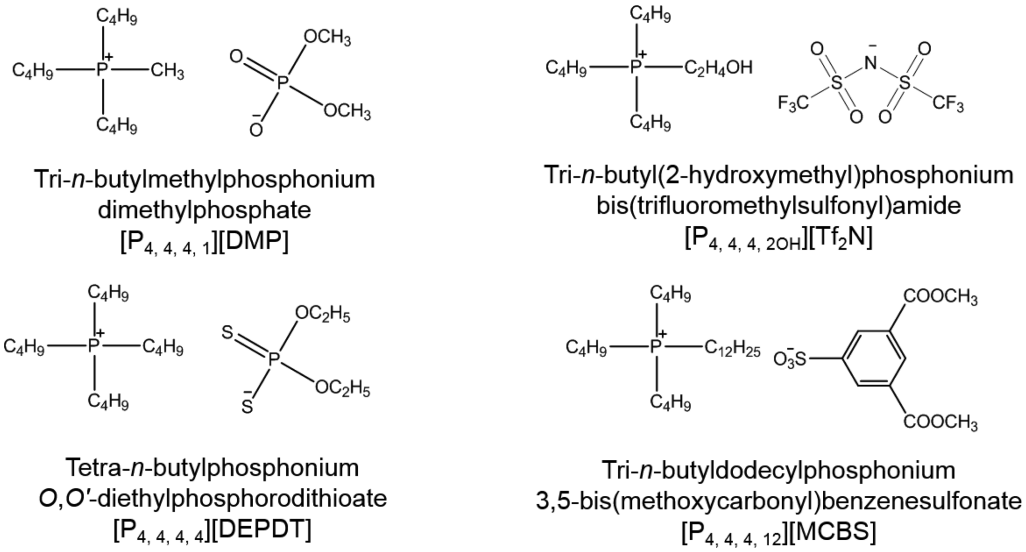

Figure 1. Chemical structures of tri-*n*-butylalkylphosphonium cation-based RTILs reported in this paper.

2. EXPERIMENTAL SECTION

2.1. Preparation of RTILs. Phosphonium RTILs were prepared by two common synthetic processes. The first process is a quaternization reaction between tri-*n*-alkylphosphine and alkyl halide to synthesize a quaternary phosphonium halide, and the second process is an anion-exchange reaction between the resulting phosphonium halide and alkali metal salt with target anion. To be more specific, for example, tri-*n*-butyl(2-hydroxymethyl)phosphonium bis(trifluoromethylsulfonyl)-amide ($[P_{4,4,4,2OH}][Tf_2N]$) was synthesized by the following procedures. The quaternization reaction between tri-*n*-butylphosphine (Nippon Chemical Industrial, ultrapure grade) and 1-bromoethanol (Tokyo Chemical Industry) was carried out at 353 K under a nitrogen atmosphere. Tri-*n*-butylphosphine was used as received. The obtained tri-*n*-butyl(2-hydroxymethyl)phosphonium bromide ($[P_{4,4,4,2OH}]Br$) was rinsed with *n*-hexane to remove unreacted tri-*n*-butylphosphine and 1-bromoethanol. The $[P_{4,4,4,2OH}]Br$ dried under vacuum and $Li[Tf_2N]$ were mixed thoroughly in ultrapure water at ambient temperature to yield the $[P_{4,4,4,2OH}]$-$[Tf_2N]$ by the anion exchange reaction; then, the crude $[P_{4,4,4,2OH}][Tf_2N]$ was extracted by toluene and purified by rinsing with ultrapure water several times until no residual bromide anion was detected with the use of 0.1 M $AgNO_3$ aqueous solution. Tetra-*n*-butylphosphonium *O,O′*-diethylphosphorodithioate ($[P_{4,4,4,4}][DEPDT]$) and tri-*n*-butyldodecylphosphonium 3,5-bis(methoxycarbonyl)benzenesulfonate ($[P_{4,4,4,12}][MCBS]$) were also prepared by the similar way previously described. Tri-*n*-butylmethylphosphonium dimethylphosphate ($[P_{4,4,4,1}][DMP]$), which was supplied by Nippon Chemical Industrial, was directly synthesized by a straightforward reaction of tri-*n*-butylphosphine with trimethylphosphate without any solvent. All RTILs employed in this study were dried at 373 K under vacuum condition (ca. 0.67 Pa) for 12 h and were stored in an argon-gas-filled glovebox prior to their characterization and physicochemical experiments. Water content of $[P_{4,4,4,1}][DMP]$, $[P_{4,4,4,2OH}][Tf_2N]$, and $[P_{4,4,4,12}]$-$[MCBS]$, determined by Karl Fischer titration, was below 40 ppm. However, that of $[P_{4,4,4,4}][DEPDT]$ could not be estimated due to an unexpected reaction with Karl Fischer solution. The obtained products were confirmed by ^1H, ^{13}C, ^{19}F, and ^{31}P NMR. NMR spectra of ^1H and ^{13}C were referred by tetramethylsilane and $CDCl_3$ as an internal reference, respectively. NMR spectra on ^{19}F and ^{31}P were measured by using trifluorotoluene and triphenyl phosphate as an external reference, respectively. Elemental composition of the RTILs was determined by elemental analyses of carbon, hydrogen, and nitrogen.

2.2. NMR Characterization and Elemental Analysis Data. Tri-*n*-butylmethylphosphonium dimethylphosphate ($[P_{4,4,4,1}][DMP]$), $(C_4H_9)_3(CH_3)P\text{-}PO_2(OCH_3)_2$. ^1H NMR (599.85 MHz in $CDCl_3$), δ 0.93−1.01 (t, 9H, $P^+CH_2(CH_2)_2CH_3$); 1.47−1.59 (m, 12H, $P^+CH_2(CH_2)_2CH_3$); 2.04−2.10 (d, 3H, P^+CH_3); 2.34−2.44 (m, 6H, $P^+CH_2(CH_2)_2CH_3$); 3.54−3.61 (d, 6H, $PO_2(OCH_3)_2^-$). ^{13}C NMR (150.85 MHz in $CDCl_3$), δ 3.9−4.4 (d, P^+CH_3); 13.37 (s, $P^+CH_2(CH_2)_2CH_3$); 19.4−19.9 (d, $P^+CH_2(CH_2)_2CH_3$); 23.4−23.9 (various d, $P^+CH_2(CH_2)_2CH_3$); 52.1−52.3 (d, $PO_2(OCH_3)_2^-$). ^{31}P NMR (242.82 MHz in $CDCl_3$), δ 2.02 (s, $PO_2(OCH_3)_2^-$); 31.81 (s, $(C_4H_9)_3(CH_3)P^+$). Elemental analysis calcd (%) for $C_{15}H_{36}O_4P_2$: C 52.62, H 10.60; found: C 52.47, H 11.06.

Tri-*n*-butyl(2-hydroxymethyl)phosphonium bis-(trifluoromethylsulfonyl)amide ($[P_{4,4,4,2OH}][Tf_2N]$), $(C_4H_9)_3(C_2H_4OH)P\text{-}N(SO_2CF_3)_2$. ^1H NMR (599.85 MHz in $CDCl_3$), δ 0.92−1.00 (t, 9H, $P^+CH_2(CH_2)_2CH_3$); 1.45−1.57 (m, 12H, $P^+CH_2(CH_2)_2CH_3$); 2.13−2.19 (m, 6H, $P^+CH_2(CH_2)_2CH_3$); 2.39−2.45 (m, 2H, $P^+CH_2CH_2OH$); 3.27−3.33 (br, 1H, $P^+CH_2CH_2OH$); 3.97−4.05 (d, 2H, $P^+CH_2CH_2OH$). ^{13}C NMR (150.85 MHz in $CDCl_3$), δ 13.14 (s, $P^+CH_2(CH_2)_2CH_3$); 19.00−19.50 (various d, $P^+CH_2(CH_2)_2CH_3$, $P^+CH_2CH_2OH$); 55.40−55.55 (d, $P^+CH_2CH_2OH$); 119.74 (q, $N(SO_2CF_3)_2^-$). ^{19}F (564.40 MHz in $CDCl_3$), δ −80.48 (s, $N(SO_2CF_3)_2^-$) ppm. ^{31}P NMR (242.82 MHz in $CDCl_3$), δ 33.02 (s, $P^+CH_2(CH_2)_2CH_3$). Elemental analysis calcd (%) for $C_{16}H_{32}F_6NO_5PS_2$: C 36.43, H 6.11, N 2.66; found: C 36.63, H 6.25, N 2.66.

Tetra-*n*-butylphosphonium *O,O′*-diethylphosphorodithioate ($[P_{4,4,4,4}][DEPDT]$), $(C_4H_9)_4P\text{-}PS_2(OC_2H_5)_2$. ^1H NMR (599.85 MHz in $CDCl_3$), δ 0.96−1.01 (t, 9H, $P^+CH_2(CH_2)_2CH_3$); 1.26−1.31 (t, 6H, $PS_2(OCH_2CH_3)_2^-$); 1.53−1.60 (m, 16H, $P^+CH_2(CH_2)_2CH_3$); 2.41−2.48 (m, 8H,

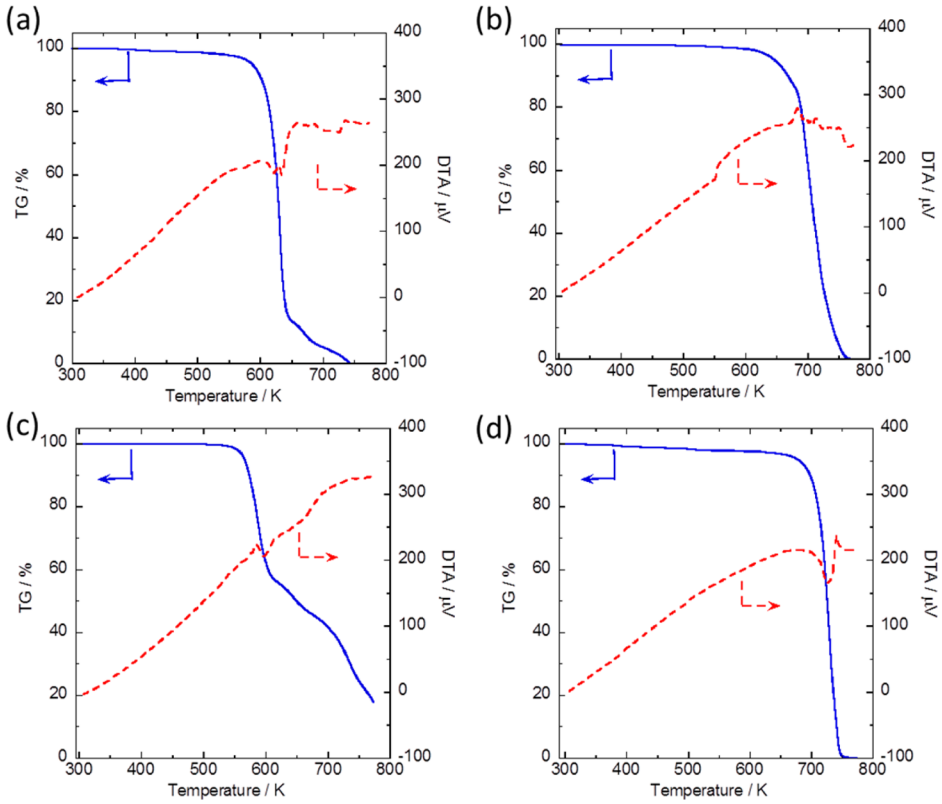

Figure 2. Results of thermogravimetry-differential thermal analysis measurement of the tri-*n*-butylalkylphosphonium cation-based RTILs. The samples were (a) $[P_{4,4,4,1}][DMP]$, (b) $[P_{4,4,4,2OH}][Tf_2N]$, (c) $[P_{4,4,4,4}][DEPDT]$, and (d) $[P_{4,4,4,12}][MCBS]$. The measurements were conducted at 10 K min^{-1}.

$P^+CH_2(CH_2)_2CH_3$); 4.03−4.09 (m, 4H, $PS_2(OCH_2CH_3)_2^-$). ^{13}C NMR (150.85 MHz in $CDCl_3$), δ 13.45 (s, $P^+CH_2(CH_2)_2CH_3$); 16.17−16.30 (d, $P^+CH_2(CH_2)_2CH_3$); 18.77−19.33 (d, $PS_2(OCH_2CH_3)_2^-$); 23.74−24.03 (m, $P^+CH_2(CH_2)_2CH_3$); 60.97−61.14 (d, $PS_2(OCH_2CH_3)_2^-$). ^{31}P NMR (242.82 MHz in $CDCl_3$), δ 32.41 (s, $(C_4H_9)_4P^+$); 112.29 (s, $PS_2(OCH_2CH_3)_2^-$). Elemental analysis calcd (%) for $C_{20}H_{46}O_2P_2S_2$: C 54.02, H 10.43; found: C 53.93, H 10.53.

Tri-*n*-butyldodecylphosphonium 3,4-bis(methoxycarbonyl)-benzenesulfonate ($[P_{4,4,4,12}][MCBS]$), $(C_4H_9)_3(C_{12}H_{25})P-C_6H_3(COOCH_3)_2(SO_3)$. ^1H NMR (599.85 MHz in $CDCl_3$), δ 0.86−0.90 (t, 3H, $P^+CH_2CH_2(CH_2)_8CH_2CH_3$); 0.92−0.99 (t, 9H, $P^+CH_2(CH_2)_2CH_3$); 1.21−1.33 (m, 16H, $P^+CH_2CH_2(CH_2)_8CH_2CH_3$); 1.40−1.58 (m, 16H, $P^+CH_2CH_2(CH_2)_8CH_2CH_3$, $P^+CH_2(CH_2)_2CH_3$); 2.25−2.37 (m, 8H, $P^+CH_2CH_2(CH_2)_8CH_2CH_3$, $P^+CH_2(CH_2)_2CH_3$); 3.92 (s, 6H, $C_6H_3(COOCH_3)_2(SO_3)^-$); 8.65 (s, 1H, $C_6H_3(COOCH_3)_2(SO_3)^-$); 8.76 (s, 2H, $C_6H_3(COOCH_3)_2(SO_3)^-$). ^{13}C NMR (150.85 MHz in $CDCl_3$), δ 13.37 (s, $P^+CH_2(CH_2)_2CH_3$); 14.06 (s, $P^+CH_2CH_2(CH_2)_8CH_2CH_3$); 18.43−19.11 (various d, $P^+CH_2(CH_2)_2CH_3$, $P^+CH_2CH_2(CH_2)_8CH_2CH_3$); 21.65−24.11, 28.82−31.94 (various s, d, $P^+CH_2(CH_2)_2CH_3$, $P^+CH_2CH_2(CH_2)_8CH_2CH_3$); 52.17 (s, $C_6H_3(COOCH_3)_2(SO_3)^-$); 130.34, 131.13, 131.55 148.18 (s, $C_6H_3(COOCH_3)_2(SO_3)^-$); 165.86 (s, $C_6H_3(COOCH_3)_2(SO_3)^-$). ^{31}P NMR (242.82 MHz in $CDCl_3$), δ 32.64 (s, $(C_4H_9)_3(C_{12}H_{25})P$). Elemental analysis calcd (%) for $C_{34}H_{61}O_7PS$: C 63.32, H 9.53; found: C 63.30, H 9.54.

2.3. Measurements of Physicochemical Properties.

Thermogravimetry-differential thermal analysis (TG-DTA) was performed by a Bruker TG-DTA2000SA apparatus under a nitrogen atmosphere at 10 K min^{-1}. Differential scanning calorimetry (DSC) was conducted using a Bruker DSC 3100SA at 5 K min^{-1}. These instruments were controlled with a Bruker MTC1000SA workstation utilizing a Bruker WS5003 software. Aluminum pan without and with aluminum top for TG-DTA and DSC, respectively, was employed, and the specimens for the thermal analysis were prepared in an argon-gas-filled glove box (Vacuum Atmosphere Company NEXUS II system, H_2O and O_2 < 1 ppm). Density measurement was carried out with a 5 mL Pyrex glass pycnometer that was calibrated by ultrapure water. Viscosity was measured with a Brookfield LVDV-II+ Pro programmable viscometer. The cone spindle was CPE-42 or CPE-52. Conductivity measurement was performed by a Horiba DS-51 digital conductivity meter with a glass conductivity cell after the cell calibration with 0.1 M KCl aqueous solution. All analyses were conducted in an argon-gas-filled glove box or by using airtight cell to avoid contamination derived from the air.

3. RESULTS AND DISCUSSION

Four types of distinctive tri-*n*-butylalkylphosphonium-based RTILs prepared in this investigation, $[P_{4,4,4,1}][DMP]$, $[P_{4,4,4,2OH}][Tf_2N]$, $[P_{4,4,4,4}][DEPDT]$, and $[P_{4,4,4,12}][MCBS]$, exhibited a liquid state at room temperature (293 K). We were able to handle them under open-air condition without any trouble, although the RTILs slightly absorbed water derived from the air. $[P_{4,4,4,2OH}][Tf_2N]$, $[P_{4,4,4,4}][DEPDT]$, and $[P_{4,4,4,12}][MCBS]$ formed biphase with water like most

Table 1. Physical and Thermal Properties of the Tri-*n*-butylalkylphosphonium Cation-Based RTILs

RTILs	FW[a]	T_g/K[b]	T_{melt}/K[b]	T_{dec}/K[c]	ρ/g cm^{-3}[d]	η/cP[e]	σ/mS cm^{-1}[f]	ref
$[P_{4,4,4,1}][Tf_2N]$	497.5	193	290	652	1.27	207	0.42	30
$[P_{4,4,4,1}][(CN)_2N]$	283.4	[g]	279	651	0.96	167	1.2	33
$[P_{4,4,4,1}][(FH)_{2.3}F]$	282.3	169	249	[g]	0.97	36	6.0	37
$[P_{4,4,4,1}][DMP]$	342.4	202	290	583, 562[h]	1.03[i]	439	0.18[i]	this work
$[P_{4,4,4,2OH}][Tf_2N]$	527.5	196		668, 646[h]	1.26[i]	242	0.48[i]	this work
$[P_{4,4,4,4}][(FH)_{2.3}F]$	324.4		239, 255	[g]	0.95	47	3.7	37
$[P_{4,4,4,4}][DEPDT]$	444.7	206		574, 566[h]	1.01[i]	1107	0.083[i]	this work
$[P_{4,4,4,8}][Tf_2N]$	595.7	183		646	1.18	250	0.27	30
$[P_{4,4,4,8}][BF_4]$	402.3	191		672	1.02	1240	0.069	30
$[P_{4,4,4,8}][PF_6]$	460.5	[g]	293	636	1.12	1720	0.047	30
$[P_{4,4,4,8}][OTf]$	464.7	193		681	1.08	778	0.087	30
$[P_{4,4,4,8}][CF_3COO]$	428.6	192		467	1.03	453	0.13	30
$[P_{4,4,4,8}][SCN]$	373.6	184		651	0.95	450	0.18	30
$[P_{4,4,4,8}][Tosyl]$	486.7	209		617	1.02	2435	0.021	30
$[P_{4,4,4,8}][(CN)_2N]$	381.6	180		653	0.95	245	0.45	33
$[P_{4,4,4,8}][(FH)_{2.3}F]$	380.6	174		[g]	0.93	74	1.5	37
$[P_{4,4,4,12}][Tf_2N]$	651.8	187	284	656	1.13	303	0.18	30
$[P_{4,4,4,12}][BF_4]$	458.5	190	293	664	0.97	1310	0.047	30
$[P_{4,4,4,12}][MCBS]$	644.9	210		698, 678[h]	1.05[i]	16401	0.0042[i]	this work
$[P_{4,4,4,allyl}][Tf_2N]$	523.6	[g]	302	692	1.26[i]	138[i]	0.64[i]	35

[a]Formula weight. [b]Glass-transition or melting temperature. [c]Thermal decomposition temperature at 10% weight loss. [d]Density at 298 K. [e]Viscosity at 298 K. [f]Conductivity at 298 K. [g]No data. [h]Thermal decomposition temperature at 5% weight loss. [i]Data were obtained at 303 K.

phosphonium cation-based RTILs reported so far, but $[P_{4,4,4,1}][DMP]$ had a water-miscible nature. It is well known that organic phosphorus salt, which consists of symmetric cation and halide anion, shows a melting point above room temperature; for example, $[P_{4,4,4,4}]Br$ melts at 375.15 K.[38] However, the melting point of $[P_{4,4,4,4}][DEPDT]$ was greatly reduced due to the asymmetric structure and the large ion volume of the $[DEPDT]^-$. It suggests that the $[DEPDT]^-$ is a useful anion for RTILs with highly symmetric cation species.

TG-DTA curves for the tri-*n*-butylalkylphosphonium-based RTILs under a nitrogen atmosphere are shown in Figure 2, and their thermal decomposition temperatures determined at 5 and 10% weight loss are given in Table 1 with the data on other phosphonium cation-based RTILs. Each RTIL used in this study showed a desirable thermal stability over 560 K. It is interesting to note that $[P_{4,4,4,12}][MCBS]$ exhibited a fairly high thermal stability among the phosphonium cation-based RTILs reported to date.[22−37] Usually phosphonium cation-based RTILs tend to indicate a good thermal stability relative to the ammonium cation-based ones with similar side chains.[31,32] The degradation pathway of phosphonium-based RTILs seems to be affected by anionic species rather than cationic species. While $[P_{4,4,4,2OH}][Tf_2N]$ and $[P_{4,4,4,12}][MCBS]$ showed a simple single-step degradation in Figure 2, the degradation for $[P_{4,4,4,1}][DMP]$ and $[P_{4,4,4,4}][DEPDT]$ proceeded by two steps. This two-step degradation behavior is consistent with a previous report on phosphonium cation-based RTILs with thermally unstable anions.[24] Long-term thermal stability of RTIL, which is an important parameter for high-temperature applications, is predicable from common TG data if the measurement condition is the same; that is, RTIL with higher decomposition temperature usually shows a better long-term thermal stability.[39,40]

DSC curves for the tri-*n*-butylalkylphosphonium-based RTILs are exhibited in Figure 3. All RTILs could keep a liquid state over a wide range of temperature. $[P_{4,4,4,1}][DMP]$ indicated a peculiar thermal phase transition behavior (Figure 3a). The crystallization was observed at 246 K after the glass transition at 202 K during the heating process from 173 K, and two endothermic peaks appeared at 279 and 290 K. These endothermic peaks should be assigned to solid−solid phase transition (279 K) and to melting (290 K). It is well-known that some RTILs have an ionic plastic crystal phase if both the cation and the anion in RTIL have spherical 3-D structure or similar configuration.[28,29,36,41−43] Several phosphonium cation-based RTILs also have such an ionic plastic crystal phase.[28,29,36] Timmermans proposed that the phase transition to the plastic crystal phase occurs by a low entropy change of fusion (ΔS_{fus} < 20 J K^{-1} mol^{-1}).[44] In regard to the $[P_{4,4,4,1}][DMP]$, the entropy changes (ΔS) of the endothermic peaks were 11.0 (enthalpy change, ΔH = 3077 J mol^{-1}) and 17.7 J K^{-1} mol^{-1} (ΔH = 5135 J mol^{-1}) at 279 and 290 K, respectively. These results suggest that the plastic crystal phase exists within a range of 279−290

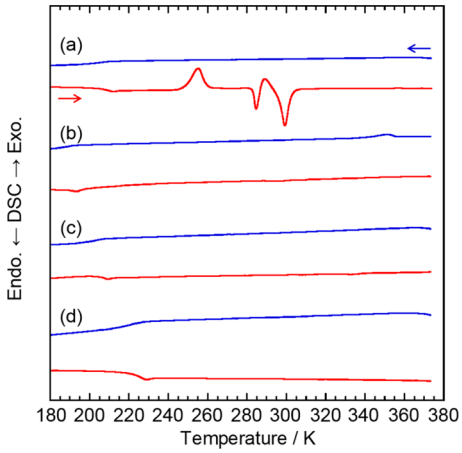

Figure 3. Differential scanning calorimetry curves of the tri-*n*-butylalkylphosphonium cation-based RTILs. The samples were (a) $[P_{4,4,4,1}][DMP]$, (b) $[P_{4,4,4,2OH}][Tf_2N]$, (c) $[P_{4,4,4,4}][DEPDT]$, and (d) $[P_{4,4,4,12}][MCBS]$. The measurements were conducted at 5 K min^{-1}.

K. Analogous ionic plastic crystal phase in a narrow temperature range has already been reported.[45−47] $[P_{4,4,4,1}]$[DMP] should be considered as a new example of RTIL with the plastic crystal phase. As for other three RTILs, $[P_{4,4,4,2OH}][Tf_2N]$, $[P_{4,4,4,4}]$[DEPDT], and $[P_{4,4,4,12}]$[MCBS], only glass-transition point appeared at 196, 206, and 210 K, respectively, during the heating process (Figure 3b−d). Although $[P_{4,4,4,4}]$[DEPDT] is composed of the cation having more spherical structure than the $[P_{4,4,4,1}]^+$ and the characteristic anion similar to $[DMP]^-$, ionic plastic crystal phase did not appear.

Figure 4 shows temperature dependence of the density, ρ (g cm^{-3}), of the tri-*n*-butylalkylphosphonium cation-based RTILs

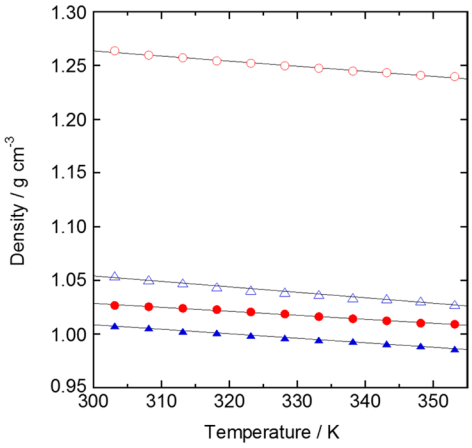

Figure 4. Temperature dependence of density of the tri-*n*-butylalkylphosphonium cation-based RTILs: (red ●) $[P_{4,4,4,1}]$[DMP], (red ○) $[P_{4,4,4,2OH}][Tf_2N]$, (blue ▲) $[P_{4,4,4,4}]$[DEPDT], and (blue △) $[P_{4,4,4,12}]$[MCBS].

depicted in Figure 1. A linear dependence with absolute temperature was obtained for all RTILs. The density is expressed as a function of temperature:

$$\rho = a + bT \tag{1}$$

where *a*, *b*, and *T* are a density at 0 K (g cm^{-3}), a coefficient of volume expansion (g cm^{-3} K^{-1}), and an absolute temperature (K), respectively. The parameters fitted by the method of least-squares are summarized in Table 2 along with the correlation

Table 2. Fitted Parameters for the Density of the Tri-*n*-butylalkylphosphonium Cation-Based RTILs

RTILs	a/g cm^{-3}	b/g cm^{-3} K^{-1}	|R|
$[P_{4,4,4,1}]$[DMP]	1.14	-3.62×10^{-4}	0.9967
$[P_{4,4,4,2OH}][Tf_2N]$	1.41	-4.74×10^{-4}	0.9947
$[P_{4,4,4,4}]$[DEPDT]	1.14	-4.24×10^{-4}	0.9985
$[P_{4,4,4,12}]$[MCBS]	1.21	-5.09×10^{-4}	0.9936

coefficient, |*R*|, for the fitting. The density decreased in the following order: $[P_{4,4,4,2OH}][Tf_2N]$, $[P_{4,4,4,12}]$[MCBS], $[P_{4,4,4,1}]$-[DMP], and $[P_{4,4,4,4}]$[DEPDT]. Optimized ionic volumes of the tri-*n*-butylalkylphosphonium cation-based RTILs calculated with the B3LYP/6-31G+(d) level using Gaussian 09 program were 574.7 Å^3 ($[P_{4,4,4,2OH}][Tf_2N]$), 800.5 Å^3 ($[P_{4,4,4,12}]$-[MCBS]), 607.2 Å^3 ($[P_{4,4,4,1}]$[DMP]), and 487.1 Å^3 ($[P_{4,4,4,4}]$-[DEPDT]).[48] These values were estimated from the sum of the individually calculated cation and anion volumes. It is reported that ionic volume in RTIL has a close relationship with physicochemical properties, which can be understood by lattice and solvation energies,[49,50] and provides useful information for prediction of physical properties, for example, viscosity, conductivity, and density.[51] With regard to the 1,3-dialkylimidazolium cation-based RTILs, the density ordinarily decreases with increasing alkyl chain length.[52] However, $[P_{4,4,4,1}]$[DMP] and $[P_{4,4,4,4}]$[DEPDT] showed smaller density values than $[P_{4,4,4,12}]$[MCBS] despite their smaller ionic volume. This result implies that the density for the RTILs is determined by both the volume of the ionic species and the local structure in RTIL that is provoked by electrostatic interaction and intermolecular electron repulsion.

Temperature dependences of the absolute viscosity, η (cP (= mPa s)), for the four RTILs are indicated in Figure 5.

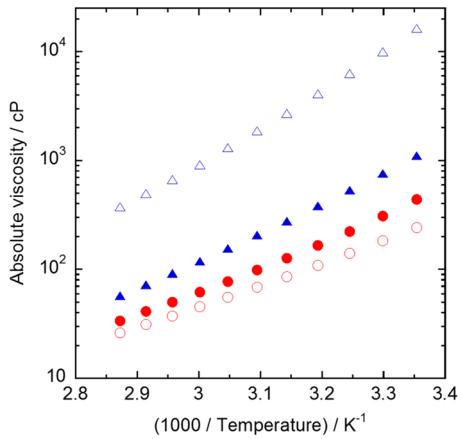

Figure 5. Arrhenius plots of absolute viscosity of the tri-*n*-butylalkylphosphonium cation-based RTILs: (red ●) $[P_{4,4,4,1}]$[DMP], (red ○) $[P_{4,4,4,2OH}][Tf_2N]$, (blue ▲) $[P_{4,4,4,4}]$[DEPDT], and (blue △) $[P_{4,4,4,12}]$[MCBS].

$[P_{4,4,4,12}]$[MCBS] was a very viscous liquid (16401 cP s at 298 K) compared with the other three RTILs. Given that several complexes with anion similar to the $[MCBS]^-$ can form a 3-D framework structure through the hydrogen bonding among the ions,[53,54] there is a high possibility that analogous framework structure is formed in the $[P_{4,4,4,12}]$[MCBS]. The structure may cause the drastic increase in the viscosity. Arrhenius plots of each viscosity indicated in Figure 5 are convex downward curves. It is a typical behavior of the glass-forming RTIL. In this case, the plots can be fitted in the Vogel−Tamman−Fulcher (VTF) equation, as expressed below, and enable further useful investigation:[55]

$$\ln \eta = \frac{k_\eta}{T - T_0} + \frac{1}{2}\ln T - \ln A_\eta \tag{2}$$

where k_η (K) is a constant related to Arrhenius activation energy for the viscous behavior, T_0 (K) is an ideal glass transition temperature, and A_η is a scaling factor. The fitted parameters are summarized in Table 3 along with the correlation coefficient, |*R*|.

Figure 6 shows temperature dependence of the ionic conductivity, σ (mS cm^{-1}), for the tri-*n*-butylalkylphosphonium-based RTILs. In general, ionic conductivity of RTIL depends on its absolute viscosity because ion mobility is restricted by the viscosity. Arrhenius-type plots of the ionic conductivity exhibited a usual behavior; that is, the plots in each RTIL are convex upward curves and the values decrease with

Table 3. Fitted Parameters for the VTF Equation of Absolute Viscosity and Equivalent Conductivity for the Tri-*n*-butylalkylphosphonium Cation-based RTILs

RTILs	absolute viscosity/cP (= mPa s)				equivalent conductivity/S cm^2 mol^{-1}			
	T_0/K	k_η/K	ln A_η	|R|	T_0/K	k_Λ/K	ln A_Λ	|R|
[$P_{4,4,4,1}$][DMP]	171	1.19×10^3	6.10	0.9999	96	2.55×10^3	6.63	0.9998
[$P_{4,4,4,2OH}$][Tf_2N]	129	1.71×10^3	7.46	0.9999	90	2.18×10^3	5.79	0.9999
[$P_{4,4,4,4}$][DEPDT]	124	2.29×10^3	9.00	0.9999	159	1.51×10^3	4.28	0.9999
[$P_{4,4,4,12}$][MCBS]	156	2.11×10^3	7.98	0.9999	158	1.75×10^3	3.66	0.9999

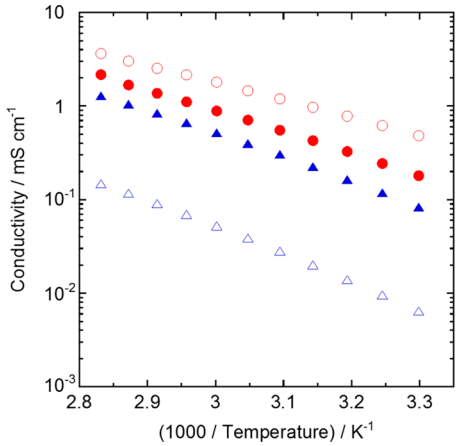

Figure 6. Arrhenius plots of conductivity of the tri-*n*-butylalkylphosphonium cation-based RTILs: (red ●) [$P_{4,4,4,1}$][DMP], (red ○) [$P_{4,4,4,2OH}$][Tf_2N], (blue ▲) [$P_{4,4,4,4}$][DEPDT], and (blue △) [$P_{4,4,4,12}$][MCBS].

decreasing temperature. As given in Table 1, the [$P_{4,4,4,2OH}$][Tf_2N] showed a relatively high conductivity among the RTILs consisting of tri-*n*-butylalkylphosphonium cation and fluoroanion except fluorohydrogenate anion because of the combination of appropriate cationic volume and flexible [Tf_2N]$^-$ anion. Interestingly the conductivity of the [$P_{4,4,4,4}$][DEPDT] was about twice as much as that of the [$P_{4,4,4,12}$][BF_4] having similar viscosity and molecular weight.[30] The experimental data of the ionic conductivity were converted to the equivalent conductivity, Λ (S cm^2 mol^{-1}), by using a following equation to fit the plot by the VTF equation and to discuss the activation energy of the equivalent conductivity.

$$\Lambda = \sigma M/\rho \tag{3}$$

where M is a formula weight of phosphonium-based RTILs. The obtained values of Λ were fitted by eq 4:

$$\ln \Lambda = -\frac{k_\Lambda}{T - T_0} - \frac{1}{2}\ln T + \ln A_\Lambda \tag{4}$$

where k_Λ (K) is a constant related to Arrhenius activation energy for the conduction behavior, T_0 (K) is an ideal glass transition temperature, and A_Λ is a scaling factor. The fitted parameters are summarized in Table 3 along with the correlation coefficient. The temperature-dependence activation energies for the absolute viscosity, $E_{a,\eta}$, and equivalent conductivity, $E_{a,\Lambda}$, can be calculated from the equation obtained by the partial differentiation on eq 2 and 4 with respect to T, as expressed below:[56,57]

$$E_{a,\eta} = -RT^2\left(\frac{\partial \ln \eta}{\partial T}\right) = \frac{Rk_\eta T^2}{(T - T_0)^2} - \frac{RT}{2} \tag{5}$$

$$E_{a,\Lambda} = RT^2\left(\frac{\partial \ln \Lambda}{\partial T}\right) = \frac{Rk_\Lambda T^2}{(T - T_0)^2} - \frac{RT}{2} \tag{6}$$

The resulting plots of $E_{a,\eta}$ and $E_{a,\Lambda}$ versus temperature are given in Figure 7. As other RTIL systems, those activation energies decreased with increasing temperature, and most values for the $E_{a,\eta}$ were larger than the $E_{a,\Lambda}$ at the same temperature.[18,58,59] However the differences between $E_{a,\eta}$ and $E_{a,\Lambda}$ were obviously larger than those for common RTILs, especially at lower

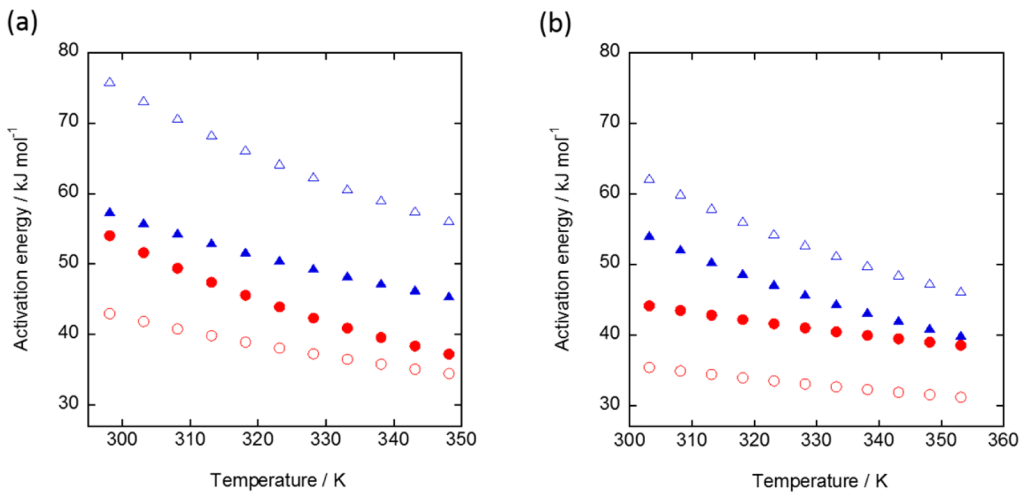

Figure 7. Temperature-dependence activation energies for (a) the absolute viscosity and (b) the equivalent conductivity for the tri-*n*-butylalkylphosphonium cation-based RTILs: (red ●) [$P_{4,4,4,1}$][DMP], (red ○) [$P_{4,4,4,2OH}$][Tf_2N], (blue ▲) [$P_{4,4,4,4}$][DEPDT], and (blue △) [$P_{4,4,4,12}$][MCBS].

temperature. Of the four tri-*n*-butylalkylphosphonium-based RTILs, $[P_{4,4,4,12}][MCBS]$ exhibited the largest difference, suggesting that it has a unique ion-conductive mechanism. In fact, the framework structure that can contribute to effective ion conduction seems to be in the $[P_{4,4,4,12}][MCBS]$, as already described in the discussion on the viscosity. The ion conduction would be controlled with the viscosity as well as the anomalous local structure in the tri-*n*-butylalkylphosphonium-based RTILs.

To investigate the correlation between conductivity and viscosity rigorously, we examined the dissociation behavior in the RTILs. It is able to be estimated in two ways. One is a recent analytical technique using a pulsed-field-gradient spin−echo (PGSE) NMR[60] and another is a classical Walden plot method constructed from fluidic properties of RTIL, that is, equivalent conductivity (S cm^2 mol^{-1}) and fluidity (reciprocal of absolute viscosity (cP^{-1})).[61] Here we used the latter approach. In this approach, diluted KCl aqueous solution is regarded as an ideal dissociation state.[61] From the difference of Walden plots between the diluted KCl aqueous solution and RTIL, we can estimate the dissociation degree and speculate the ion conduction behavior in the RTILs. Also, we may apply "hole theory" to our physical data to discuss them more precisely,[62] but in this study we employed the ideal KCl line to simplify the estimation and the speculation. The Walden plot of the tri-*n*-butylalkylphosphonium-based RTILs in this study is shown in Figure 8, with that of other RTILs given in Table 1.

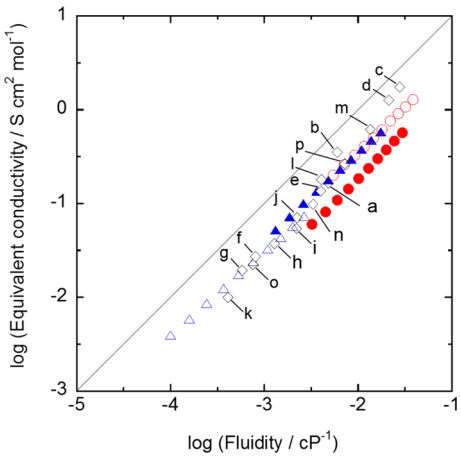

Figure 8. Walden plots of the phosphonium cation-based RTILs: (red ●) $[P_{4,4,4,1}][DMP]$, (red ○) $[P_{4,4,4,2OH}][Tf_2N]$, (blue ▲) $[P_{4,4,4,4}][DEPDT]$, (blue △) $[P_{4,4,4,12}][MCBS]$, (a): $[P_{4,4,4,1}][Tf_2N]$, (b): $[P_{4,4,4,1}][(CN)_2N]$, (c): $[P_{4,4,4,1}][(FH)_{2.3}F]$, (d): $[P_{4,4,4,4}][(FH)_{2.3}F]$, (e): $[P_{4,4,4,8}][Tf_2N]$, (f): $[P_{4,4,4,8}][BF_4]$, (g): $[P_{4,4,4,8}][PF_6]$, (h): $[P_{4,4,4,8}][OTf]$, (i): $[P_{4,4,4,8}][CF_3COO]$, (j): $[P_{4,4,4,8}][SCN]$, (k): $[P_{4,4,4,8}][Tosyl]$, (l): $[P_{4,4,4,8}][(CN)_2N]$, (m): $[P_{4,4,4,8}][(FH)_{2.3}F]$, (n): $[P_{4,4,4,12}][Tf_2N]$, (o): $[P_{4,4,4,12}][BF_4]$, and (p): $[P_{4,4,4,allyl}][Tf_2N]$. The ideal line was constructed from the data for a diluted KCl aqueous solution.

Each plot was below the ideal line. The RTILs with $[(CN)_2N]^-$ and $[(FH)_{2.3}F]^-$ exhibited small deviations from the ideal line compared with other RTILs. The $[P_{4,4,4,2OH}][Tf_2N]$ and $[P_{4,4,4,4}][DEPDT]$ showed almost the same deviation from the ideal line, and it was similar to $[P_{4,4,4,1}][Tf_2N]$, $[P_{4,4,4,8}][Tf_2N]$, $[P_{4,4,4,8}][SCN]$, $[P_{4,4,4,12}][Tf_2N]$, and $[P_{4,4,4,allyl}][Tf_2N]$. We concluded that these RTILs have the similar dissociation degree and ion-conduction behavior. In other words, it suggests that the $[DEPDT]^-$ has a potential to be a useful anion in RTIL as an alternative to $[Tf_2N]^-$, which is one of the valuable anions. The dissociation degree of $[P_{4,4,4,12}][MCBS]$ seems to be slightly worse than that of the aforementioned seven RTILs but was close to $[P_{4,4,4,8}][CF_3COO]$, $[P_{4,4,4,8}][PF_6]$, $[P_{4,4,4,8}][OTf]$, $[P_{4,4,4,8}][BF_4]$, $[P_{4,4,4,8}][Tosyl]$, and $[P_{4,4,4,12}][BF_4]$. The $[P_{4,4,4,12}][MCBS]$ showed a relatively good dissociation degree, while it has a very high-viscosity. It would be due to the anomalous framework structure in the $[P_{4,4,4,12}][MCBS]$, as already stated. As for the $[P_{4,4,4,1}][DMP]$, there was a considerable deviation. It is highly likely that the dissociation is insufficient or the associated ions exist in this RTIL system.

4. CONCLUSIONS

We examined the physicochemical properties of the distinctive tri-*n*-butylalkylphosphonium-based RTILs. All RTILs prepared in this investigation indicated a favorable thermal decomposition temperature exceeding 560 K. The $[P_{4,4,4,12}][MCBS]$ had a fairly high thermal stability, and several unique physicochemical behaviors in the RTIL were revealed. The physicochemical behavior would be caused by the anomalous framework structure in the RTIL. The $[P_{4,4,4,1}][DMP]$ formed an ionic plastic crystal phase, but for $[P_{4,4,4,4}][DEPDT]$ with the ion structures similar to $[P_{4,4,4,1}]^+$ and $[DMP]^-$ this was not the case. The $[P_{4,4,4,2OH}][Tf_2N]$ showed a relatively high conductivity among the tri-*n*-butylalkylphosphonium-based RTILs with usual fluoroanion. There is no doubt that the anion structure in the phosphonium cation-based RTILs strongly affect the thermal stability and the phase-transition properties. These results will be useful information if a novel functional phosphonium-based RTIL system is designed.

■ AUTHOR INFORMATION

Corresponding Authors

*Tel/Fax: +81-6-6879-7374. E-mail: ttsuda@chem.eng.osaka-u.ac.jp (T.T.).

*E-mail: kuwabata@chem.eng.osaka-u.ac.jp (S.K.).

Notes

The authors declare no competing financial interest.

■ ACKNOWLEDGMENTS

K.Y. thanks Japan Society for the Promotion of Science (JSPS) for the research fellowship. Part of this research was supported by Grant-in-Aid for Scientific Research B, Grant No. 24350071 from the Japanese Ministry of Education, Culture, Sports, Science and Technology (MEXT), and Advanced Low Carbon Technology (ALCA) Research and Development Program from Japan Science and Technology Agency (JST). We thank Dr. K. Inoue (Chemical Analysis Center, Graduate School of Engineering, Osaka University) for her help on the NMR measurements. Nippon Chemical Industrial Co., Ltd. provided some chemicals including RTILs free of charge.

■ REFERENCES

(1) Plechkova, N. V.; Seddon, K. R. Applications of Ionic Liquids in the Chemical Industry. *Chem. Soc. Rev.* **2008**, *37*, 123−150.

(2) Armand, M.; Endres, F.; MacFarlane, D. R.; Ohno, H.; Scrosati, B. Ionic-liquid Materials for the Electrochemical Challenges of the Future. *Nat. Mater.* **2009**, *8*, 621−629.

(3) Ma, Z.; Yu, J.-H.; Dai, S. Preparation of Inorganic Materials Using Ionic Liquids. *Adv. Mater.* **2010**, *22*, 261−285.

(4) Kuwabata, S.; Tsuda, T.; Torimoto, T. Room-Temperature Ionic Liquid. A New Medium for Material Production and Analyses under Vacuum Conditions. *J. Phys. Chem. Lett.* **2010**, 3177−3188.
(5) Torimoto, T.; Tsuda, T.; Okazaki, K.; Kuwabata, S. New Frontiers in Materials Science Opened by Ionic Liquids. *Adv. Mater.* **2010**, *22*, 1196−1221.
(6) Endres, F.; Abbott, A. P.; MacFarlane, D. R. *Electrodeposition from Ionic Liquids*; Wiley-VCH: Weinheim, Germany, 2008.
(7) Galinski, M.; Lewandowski, A.; Stepniak, I. Ionic Liquids as Electrolytes. *Electrochim. Acta* **2006**, *51*, 5567−5580.
(8) Pârvulescu, V. I.; Hardacre, C. Catalysis in Ionic Liquids. *Chem. Rev.* **2007**, *107*, 2615−2665.
(9) Hapiot, P.; Lagrost, C. Electrochemical Reactivity in Room-Temperature Ionic Liquids. *Chem. Rev.* **2008**, *108*, 2238−2264.
(10) Wang, H.; Gurau, G.; Rogers, R. D. Ionic Liquid Processing of Cellulose. *Chem. Soc. Rev.* **2012**, *41*, 1519−1537.
(11) Sun, X.-Q.; Luo, H.-M.; Dai, S. Ionic Liquids-Based Extraction: A Promising Strategy for the Advanced Nuclear Fuel Cycle. *Chem. Rev.* **2012**, *112*, 2100−2128.
(12) Wilkes, J. S.; Zaworotko, M. J. Air and Water Stable 1-Ethyl-3-Methylimidazolium Based Ionic Liquids. *Chem. Commun.* **1992**, 965−967.
(13) Cooper, E. I. *Proceedings of the Eighth International Symposium on Molten Salts*; Gale, R. J.; Blomgren, G.; Kojima, H., Eds.; The Electrochemical Society: Pennington, NJ, 1992; Vol. *92-16*, p 386.
(14) Zhang, S.-J.; Lu, X.-M.; Zhou, Q.; Li, X.-H.; Zhang, X.-P.; Li, S.-C. *Ionic Liquids*; Elsevier: Amsterdam, 2009.
(15) Ahrens, S.; Peritz, A.; Strassner, T. Tunable Aryl Alkyl Ionic Liquids (TAAILs): The Next Generation of Ionic Liquids. *Angew. Chem., Int. Ed.* **2009**, *48*, 7908−7910.
(16) Tsuda, T.; Kondo, K.; Tomioka, T.; Takahashi, Y.; Matsumoto, H.; Kuwabata, S.; Hussey, C. L. Design, Synthesis, and Electrochemistry of Room-Temperature Ionic Liquids Functionalized with Propylene Carbonate. *Angew. Chem., Int. Ed.* **2011**, *50*, 1310−1313.
(17) Yoshida, K.; Nakamura, M.; Kazue, Y.; Tachikawa, N.; Tsuzuki, S.; Seki, S.; Dokko, K.; Watanabe, M. Oxidative-Stability Enhancement and Charge Transport Mechanism in Glyme-Lithium Salt Equimolar Complexes. *J. Am. Chem. Soc.* **2011**, *133*, 13121−13129.
(18) Tsuda, T.; Kondo, K.; Baba, M.; Suwa, S.; Ikeda, Y.; Sakamoto, T.; Seino, S.; Yoshida, H.; Ozaki, M.; Imanishi, A.; Kuwabata, S. Physicochemical Properties of 1-alkyl-3-Methylimidazolium chloride−urea Melts. *Electrochim. Acta* **2013**, *100*, 285−292.
(19) Joshi, M. D.; Chalumot, G.; Kim, Y.; Anderson, J. L. Synthesis of Glucaminium-based Ionic Liquids and their Application in the Removal of Boron from Water. *Chem. Commun.* **2012**, *48*, 1410−1412.
(20) Majhi, P. K.; Sauerbrey, S.; Schnakenburg, G.; Arduengo, A. J.; Streubel, R. Synthesis of Backbone *P*-Functionalized Imidazol-2-ylidene Complexes: En Route to Novel Functional Ionic Liquids. *Inorg. Chem.* **2012**, *51*, 10408−10416.
(21) Tsuda, T.; Hussey, C. L. *Modern Aspects of Electrochemistry*, Vol. *45*; White, R. E., Ed.; Springer Science+Business Media: New York, 2009; p 63.
(22) Del Sesto, R. E.; Corley, C.; Robertson, A.; Wilkes, J. S. Tetraalkylphosphonium-based Ionic Liquids. *J. Organomet. Chem.* **2005**, *690*, 2536−2542.
(23) Fraser, K. J.; Izgorodina, E. I.; Forsyth, M.; Scott, J. L.; MacFarlane, D. R. Liquids Intermediate between "Molecular" and "Ionic" Liquids: Liquid Ion Pairs? *Chem. Commun.* **2007**, 3817−3819.
(24) Green, M. D.; Schreiner, C.; Long, T. E. Thermal, Rheological, and Ion-Transport Properties of Phosphonium-Based Ionic Liquids. *J. Phys. Chem. A* **2011**, *115*, 13829−13835.
(25) Bradaric, C. J.; Downard, A.; Kennedy, C.; Robertson, A. J.; Zhou, Y.-H. Industrial Preparation of Phosphonium Ionic Liquids. *Green Chem.* **2003**, *5*, 143−152.
(26) Fukumoto, K.; Ohno, H. LCST-Type Phase Changes of a Mixture of Water and Ionic Liquids Derived from Amino Acids. *Angew. Chem., Int. Ed.* **2007**, *46*, 1852−1855.
(27) Tsuji, Y.; Ohno, H. Facile Preparation of Hydroxide Ion or Proton Conductive Ionic Liquids by Mixing Tetra-*n*-butylphosphonium Hydroxide and Benzimidazole. *RSC Adv.* **2012**, *2*, 11279−11284.
(28) Armel, V.; Velayutham, D.; Sun, J.-Z.; Howlett, P. C.; Forsyth, M.; MacFarlane, D. R.; Pringle, J. M. Ionic Liquids and Organic Ionic Plastic Crystals Utilizing Small Phosphonium Cations. *J. Mater. Chem.* **2011**, *21*, 7640−7650.
(29) Jin, L.; Nairn, K. M.; Forsyth, C. M.; Seeber, A. J.; MacFarlane, D. R.; Howlett, P. C.; Forsyth, M.; Pringle, J. M. Structure and Transport Properties of a Plastic Crystal Ion Conductor: Diethyl-(methyl)(isobutyl)phosphonium Hexafluorophosphate. *J. Am. Chem. Soc.* **2012**, *134*, 9688−9697.
(30) Tsunashima, K.; Sugiya, M. Physical and Electrochemical Properties of Room-Temperature Dicyanamide Ionic Liquids Based on Quaternary Phosphonium Cations. *Electrochemistry* **2007**, *75*, 734−736.
(31) Tsunashima, K.; Sugiya, M. Physical and Electrochemical Properties of Low-viscosity Phosphonium Ionic Liquids as Potential Electrolytes. *Electrochem. Commun.* **2007**, *9*, 2353−2358.
(32) Tsunashima, K.; Niwa, E.; Kodama, S.; Sugiya, M.; Ono, Y. Thermal and Transport Properties of Ionic Liquids Based on Benzyl-Substituted Phosphonium Cations. *J. Phys. Chem. B* **2009**, *113*, 15870−15874.
(33) Tsunashima, K.; Kodama, S.; Sugiya, M.; Kunugi, Y. Physical and Electrochemical Properties of Room-temperature Dicyanamide Ionic Liquids Based on Quaternary Phosphonium Cations. *Electrochim. Acta* **2010**, *56*, 762−766.
(34) Tsunashima, K.; Kawabata, A.; Matsumiya, M.; Kodama, S.; Enomoto, R.; Sugiya, M.; Kunugi, Y. Low Viscous and Highly Conductive Phosphonium Ionic Liquids Based on Bis(fluorosulfonyl)-amide Anion as Potential Electrolytes. *Electrochem. Commun.* **2011**, *13*, 178−181.
(35) Tsunashima, K.; Ono, Y.; Sugiya, M. Physical and Electrochemical Characterization of Ionic Liquids Based on Quaternary Phosphonium Cations Containing a Carbon−carbon Double Bond. *Electrochim. Acta* **2011**, *56*, 4351−4355.
(36) Enomoto, T.; Kanematsu, S.; Tsunashima, K.; Matsumoto, K.; Hagiwara, R. Physicochemical Properties and Plastic Crystal Structures of Phosphonium Fluorohydrogenate Salts. *Phys. Chem. Chem. Phys.* **2011**, *13*, 12536−12544.
(37) Kanematsu, S.; Matsumoto, K.; Hagiwara, R. Electrochemically Stable Fluorohydrogenate Ionic Liquids Based on Quaternary Phosphonium Cations. *Electrochem. Commun.* **2009**, *11*, 1312−1315.
(38) Lazzús, J. A. A Group Contribution Method to Predict the Melting Point of Ionic Liquids. *Fluid Phase Equilib.* **2012**, *313*, 1−6.
(39) Wooster, T. J.; Johanson, K. M.; Fraser, K. J.; MacFarlane, D. R.; Scott, J. L. Thermal Degradation of Cyano Containing Ionic Liquids. *Green Chem.* **2006**, *8*, 691−696.
(40) Luo, H.; Baker, G. A.; Lee, J. S.; Pagni, R. M.; Dai, S. Ultrastable Super-Derived Protic Ionic Liquids. *J. Phys. Chem. B* **2009**, *113*, 4181−4183.
(41) MacFarlane, D. R.; Meakin, P.; Sun, J.; Amini, N.; Forsyth, M. Pyrrolidinium Imides: A New Family of Molten Salts and Conductive Plastic Crystal Phases. *J. Phys. Chem. B* **1999**, *103*, 4164−4170.
(42) Zhou, Z.-B.; Matsumoto, H. Lithium-doped, Organic Ionic Plastic Crystal Electrolytes Exhibiting High Ambient-temperature Conductivities. *Electrochem. Commun.* **2007**, *9*, 1017−1022.
(43) Taniki, R.; Matsumoto, K.; Hagiwara, R.; Hachiya, K.; Morinaga, T.; Sato, T. Highly Conductive Plastic Crystals Based on Fluorohydrogenate Anions. *J. Phys. Chem. B* **2013**, *117*, 955−960.
(44) Timmermans, J. Plastic Crystals: A Historical Review. *J. Phys. Chem. Solids* **1961**, *18*, 1−8.
(45) Abu-Lebdeh, Y.; Abouimrane, A.; Alarco, P.-J.; Armand, M. Ionic liquid and Plastic Crystalline Phases of Pyrazolium Imide Salts as Electrolytes for Rechargeable Lithium-Ion Batteries. *J. Power Sources* **2006**, *154*, 255−261.
(46) Zhou, Z.-B.; Matsumoto, H.; Tatsumi, K. Cyclic Quaternary Ammonium Ionic Liquids with Perfluoroalkyltrifluoroborates: Syn-

thesis, Characterization, and Properties. *Chem.—Eur. J.* **2006**, *12*, 2196−2212.
(47) Golding, J.; Forsyth, S.; MacFarlane, D. R.; Forsyth, M.; Deacon, G. B. Methanesulfonate and *p*-toluenesulfonate Salts of the *N*-methyl-*N*-alkylpyrrolidinium and Quaternary Ammonium cations: Novel Low Cost Ionic Liquids. *Green Chem.* **2002**, *4*, 223−229.
(48) Frisch, M. J.; et al. *Gaussian 09*, revision A. 02; Gasussian, Inc.: Wallingford, CT, 2009.
(49) Jenkins, H. D. B.; Roobottom, H. K.; Passmore, J.; Glasser, L. Relationships among Ionic Lattice Energies, Molecular (Formula Unit) Volumes, and Thermochemical Radii. *Inorg. Chem.* **1999**, *38*, 3609−3620.
(50) Krossing, I.; Slattery, J. M.; Daguenet, C.; Dyson, P. J.; Oleinikova, A.; Weingärtner, H. Why are Ionic Liquids Liquid? A Simple Explanation Based on Lattice and Solvation energies. *J. Am. Chem. Soc.* **2006**, *128*, 13427−13434.
(51) Slattery, J. M.; Daguenet, C.; Dyson, P. J.; Schubert, T. J. S.; Krossing, I. How to Predict the Physical Properties of Ionic Liquids: A Volume-Based Approach. *Angew. Chem., Int. Ed.* **2007**, *46*, 5384−5388.
(52) Tokuda, H.; Hayamizu, K.; Ishii, K.; Susan, M. A. B. H.; Watanabe, M. Physicochemical Properties and Structures of Room Temperature Ionic Liquids. 2. Variation of Alkyl Chain Length in Imidazolium Cation. *J. Phys. Chem. B* **2005**, *109*, 6103−6110.
(53) Novozhilova, N. V.; Magomedova, N. S.; Sobolev, A. N.; Bel'skii, V. K. Crystal and Molecular Structure of the Hydroxonium Salt of Sulfoisophthalic Acid. *J. Struct. Chem* **1989**, *30*, 515−518.
(54) Sun, D.-F.; Cao, R.; Sun, Y.-Q.; Li, X.; Bi, W.-H.; Hong, M.-C.; Zhao, Y.-J. Two New Zeolite-Like Supramolecular Copper Complexes. *Eur. J. Inorg. Chem.* **2003**, *2003*, 94−98.
(55) Angell, C. A.; Moynihan, C. T. *Molten Salts Characterization and Analysis*; Marcel Dekker: New York, 1969; p 315.
(56) Angell, C. A. Free Volume Model for Transport in Fused Salts: Electrical Conductance in Glass-Forming Nitrate Melts. *J. Phys. Chem.* **1964**, *68*, 1917−1929.
(57) Moynihan, C. T.; Angell, C. A. Mass Transport in Ionic Melts at Low Temperatures. Chronopotentiometric Diffusion Coefficients of Silver(I), Cadmium(II), and Thallium(I) in Calcium Nitrate Tetrahydrate. *J. Phys. Chem.* **1970**, *74*, 736−742.
(58) Chen, P.-Y.; Hussey, C. L. Electrodeposition of Cesium at Mercury Electrodes in the Tri-1-butylmethylammonium bis-((trifluoromethyl)sulfonyl)imide room-temperature Ionic Liquid. *Electrochim. Acta* **2004**, *49*, 5125−5138.
(59) Tsuda, T.; Boyd, L. E.; Kuwabata, S.; Hussey, C. L. Electrochemistry of Copper(I) Oxide in the 66.7−33.3 mol % Urea−Choline Chloride Room-Temperature Eutectic Melt. *J. Electrochem. Soc.* **2010**, *157*, F96−F103.
(60) Tokuda, H.; Hayamizu, K.; Ishii, K.; Susan, M. A. B. H.; Watanabe, M. Physicochemical Properties and Structures of Room Temperature Ionic Liquids. 1. Variation of Anionic Species. *J. Phys. Chem. B* **2004**, *108*, 16593−16600.
(61) Xu, W.; Cooper, E. I.; Angell, C. A. Ionic Liquids: Ion Mobilities, Glass Temperatures, and Fragilities. *J. Phys. Chem. B* **2003**, *107*, 6170−6178.
(62) MacFarlane, D. R.; Forsyth, M.; Izgorodina, E. I.; Abbott, A. P.; Annat, G.; Fraser, K. On the Concept of Ionicity in Ionic Liquids. *Phys. Chem. Chem. Phys.* **2009**, *11*, 4962−4967.